Progress in Organic Coatings 172 (2022) 107135

Contents lists available at ScienceDirect

Progress in Organic Coatings

journal homepage: www.elsevier.com/locate/porgcoat

# Anti-viral organic coatings for high touch surfaces based on smart-release, $Cu^{2+}$ containing pigments

Zack Saud [a], Calvin A.J. Richards [b], Geraint Williams [b], Richard J. Stanton [a,*]

[a] Infection and Immunity, Medicine, Cardiff University, Heath Park, Cardiff CF11 9HH, UK
[b] Department of Materials Science and Engineering, Faculty of Science and Engineering, Bay Campus, Swansea University Crymlyn Burrows, Swansea SA1 8EN, UK

ARTICLE INFO

*Keywords:*
SARS-CoV-2
Organic coating
Anti-viral
Copper
Covid19
Smart-release

ABSTRACT

Viruses such as SARS-CoV-2 can remain viable on solid surfaces for up to one week, hence fomites are a potential route of exposure to infectious virus. Copper has well documented antiviral properties that could limit this problem, however practical deployment of copper surfaces has been limited due to the associated costs and the incompatibility of copper metal in specific environments and conditions. We therefore developed an organic coating containing an intelligent-release $Cu^{2+}$ pigment based on a cation exchange resin. Organic coatings containing a 50 % weight or higher loading of smart-release pigment were capable of completely inactivating (>6 log reduction in titre) SARS-CoV-2 within 4 h of incubation. Importantly these organic coatings demonstrated a significantly enhanced ability to inactivate SARS-CoV-2 compared to metallic copper and un-pigmented material. Furthermore, the presence of contaminating proteins inhibited the antiviral activity of metallic copper, but the intelligent-release $Cu^{2+}$ pigment was unaffected. The approach of using a very basic paint system, based on a polymer binder embedded with "smart release" pigment containing an anti-viral agent which is liberated by ion-exchange, holds significant promise as a cost effective and rapidly deployed coating to confer virus inactivating capability to high touch surfaces.

## 1. Introduction

As the world continues to live through the covid 19 pandemic [1], it is clear that any means which could reduce the spread of highly infectious diseases are of great significance. Although the primary modes of transmission for SARS-CoV-2 is by airborne droplets and direct contact (physical or close contact with an infected host) [2–8], indirect contact with a fomite remains an important consideration as it has been reported that the virus can remain viable on surfaces for up to 72 h [8–10] and transfer to skin upon contact [11,12].

The anti-microbial and, more significantly, antiviral properties of copper (Cu) have been well documented in the scientific literature [13–17]. However, the practicality of deploying Cu metal or depositing metallic Cu coatings to surfaces is limited on account of the associated cost and incompatibility of Cu metal to specific environments and conditions. As such, a more convenient approach may be one where the copper is employed as an additive in a paint system, consisting of pigment, binder and solvent, which can be applied as an organic coating to potential high-touch surfaces. Several candidate technologies have been investigated as possible anti-viral coating additives, including copper iodide nanoparticles [16], cationic copper impregnated fibres [18], organo-metallic $Cu^{2+}$ complexes [19], copper (I) oxide particles [20,21] and microporous aluminosilicate zeolite materials containing copper ions [22,23]. Indeed, it was recently reported that powder coatings containing zeolite particles which had been loaded with a combination of silver, copper and zinc cations demonstrate significant anti-microbial properties [24]. An added attraction of in-coating cation-exchange materials such as zeolites is the ability to act as intelligent-release pigments, where the stored, in-coating cations remain immobilised until an environment containing other aqueous cations contacts the coating surface.

In this work we demonstrate that smart-release pigment technology, which has previously been developed for corrosion protection within organic coatings, can be adapted for anti-viral applications. Anti-corrosion pigments based on both inorganic clay materials [25–27] and organic cation-exchange resins containing stored cationic inhibitors [28,29] have previously been shown to significantly retard rates of corrosion-driven organic coating failure on steel surfaces. The technology is significantly more versatile than current state-of-the-art inhibitive pigments based on sparingly soluble salts, in that a wide range of

* Corresponding author.
*E-mail address:* stantonrj@cardiff.ac.uk (R.J. Stanton).

https://doi.org/10.1016/j.porgcoat.2022.107135
Received 24 June 2022; Received in revised form 16 August 2022; Accepted 17 August 2022

cationic corrosion inhibitors such as rare earth metal, group II, and zinc cations can be deployed using the same ion-exchange pigment system. Cation inhibitor release is triggered by the presence of cations associated with a corrosive aqueous environment, leading to inhibition of corrosion in coating defects when the underlying metal is exposed.

Here we extend this work to demonstrate a simple, cheap, yet highly effective anti-viral organic coating containing a pigment prepared from $Cu^{2+}$-loaded cation exchange resin dispersed in a polymer (polyvinyl *co* butyral-co-vinyl alcohol-co-vinyl acetate [PVB]) binder and applied to stainless steel surfaces. These organic coatings offer a significantly enhanced ability to inactivate SARS-CoV-2 compared to metallic copper and un-pigmented PVB, and are more resistant to inhibition by soil loads, making them ideal coatings for high-touch surfaces where viral transmission between individuals may occur.

## 2. Materials and methods

### 2.1. Materials

The African green monkey kidney Vero E6 cell line was obtained from American Type Culture Collection (ATCC, no. 1586). To enhance virus entry (>1-log) and generate a more sensitive assay for virucidal activity, the cell line was transduced with Lentivirus vectors expressing ACE2 and TMPRSS2 and subsequently drug selected [30]. The cells were maintained in Dulbecco's Modified Eagle's Medium - high glucose (DMEM) supplemented with 10 % fetal calf serum (FCS, Sigma Aldrich) at 37 ℃ in a humidified atmosphere of 5 % $CO_2$. SARS-CoV-2 strain England2 was propagated in the Vero E6 cells expressing ACE2 and TMPRSS2 (Vero A/T), and harvested from the supernatant which contained either 0 % or 2 % FCS (depending on the experiment). Viral titre was determined using a standard plaque assay. 100 μL of virus solution was deposited on each surface and incubated for 4 h within a biosafety cabinet, after which the spot had completely dried. The dried spot was retrieved by washing ten times with 1 mL of DMEM and 100 μL of this solution was subjected to serial dilution. All infection experiments were carried out in Cardiff University's designated biosafety level-3 (BSL-3) laboratory. Viral infections were performed in DMEM containing 2 % FCS. All relevant chemicals were purchased from Sigma Aldrich and all metal coupons were purchased from Goodfellow Metals.

### 2.2. Preparation of $Cu^{2+}$ exchanged pigment

Amberlite 120 $H^+$ has a quoted exchange capacity and density of 1.8 eq $l^{-1}$ and 1.5 kg $l^{-1}$ respectively. From these values the exchange capacity of the resin was estimated to be 1.5 milliequivalents (mEq) per gram. Based on this value, an excess of $Cu^{2+}$ was used to ensure resin saturation (calculated maximum of 9.5 g per 100 g of resin). Thus, 0.2 M of $CuSO_4.5H_2O$ was dissolved in 1 L of distilled water and 100 g of Amberlite 120 $H^+$ resin beads were added. This mixture was then stirred at a constant speed for 2 h using a magnetic stirrer. After the 2 h exchange period, the resin beads were collected using a Buchner filtration flask, washed with 500 mL of deionised water, and then dried for 24 h at 40 °C under vacuum. Once dried, the exchanged Amberlite 120 $H^+$ resin beads were milled using a Retsch planetary ball mill at 350 RPM for 2 h. The resulting powder was then sieved through a 20 μm mesh, yielding a finely-divided, light blue coloured pigment.

### 2.3. Spectrophotometric determination of Cu(II) species

The concentration of Cu ions in solution was determined by optical absorbance measurements using a PerkinElmer Lambda 750 UV/VIS/NIR Spectrometer in conjunction with 1 cm plastic cuvettes. Absorbance values for corresponding Cu concentrations were determined using a well-known methodology, whereby an excess of ammonia in solution complexes with $Cu^{2+}$ cations, forming the complex ion tetraamminecopper(II) ($Cu(NH_3)_4^{2+}$), which produces a deep blue colour [31–33]. A calibration curve was prepared by plotting the absorbance measured at $\lambda_{max} = 606$ nm as a function of known Cu concentrations between $1 \times 10^{-3}$ and $2 \times 10^{-2}$ M. The resulting plot was a good straight line ($R^2 = 0.9978$) implying that aqueous $Cu^{2+}$ solutions (between concentrations of $1 \times 10^{-3}$ and $2 \times 10^{-2}$ M) obey the Beer-Lambert law, Eq. (1).

$$A_{606} = \varepsilon_{606}\, c\, l \tag{1}$$

where $\varepsilon_{606}$ is the molar extinction coefficient at 606 nm, $c$ is concentration in M and $l$ is the optical path length in cm. The value of $\varepsilon_{606}$ obtained from the least-squares analysis of absorbance data was 42 $M^{-1}$ $cm^{-1}$ (±3) at ~20 °C, which is in good agreement with other reported values. Thereafter, the solution concentration of $Cu^{2+}$ was determined by withdrawing an aliquot, volumetrically diluting with distilled water (if necessary), mixed with an equal volume of 1 M of ammonia and measuring the absorbance at 606 nm. Measurements of the post exchange solution to estimate the amount of $Cu^{2+}$ taken up by the ion exchange resin were made by withdrawing and aliquot after the 2 H exchange period, diluted by an order of magnitude and mixing with an equal volume of 1 M ammonia. The back exchange measurements were produced by stirring 1 g of milled pigment in 10 $cm^3$ of 0.3 M $H_2SO_4$ (to ensure the most efficient back-exchange) for 2 h, the pigment was then separated from the solution by use of a centrifuge. An aliquot was removed from the solution, diluted, and prepared in the same manner as above.

### 2.4. Preparation and application of $Cu^{2+}$ exchanged pigment polymer coatings

2 cm × 2 cm 430 stainless steel substrate surfaces were prepared by abrading with 24,000 grit silicon carbide papers to remove the as-received surface, including any contaminants and/or pre-existing oxide layer. Degreasing was carried out by an acetone rinse followed by air-drying. PVB solutions (MW ~70,000–100,000) were prepared in ethanol (16 % w/w), the $Cu^{2+}$ exchanged pigment was added at known weights (0.5–5 g of pigment to 25 g of ethanolic PVB solutions) and thoroughly dispersed using a shear mixer. Organic coatings (films) were produced by bar casting the PVB-$Cu^{2+}$ exchanged pigment dispersions onto the 430 stainless steel substrates using electrical tape (~145 μm in thickness) as a height guide. Subsequent evaporation of the ethanol solvent resulted in a dry film thickness of ~25 μm (measured by a micrometre screw gauge) and a range of composite organic coating pigment loadings of 11 to 55 wt%.

### 2.5. Evaluation of antiviral activities of the $Cu^{2+}$ exchanged pigment polymer coatings and analogues

The antiviral response of the $Cu^{2+}$ exchanged pigmented coatings (hereafter referred to as CEP), pure copper powder pigmented coating (prepared in the same manner as described for the $Cu^{2+}$ exchanged coatings, at a loading of 10 g of powder to 25 g of ethanolic PVB solution), unpigmented PVB coating, bare stainless steel substrates, and bare copper substrates were all measured as follows. 100 μL of SARS-CoV2 at a titre of approximately $4 \times 10^8$ PFU/mL was applied to each sample contained within a 6 well plate and dried within a Biosafety cabinet for 4 h. After incubation, residual virus was recovered by washing with DMEM, and titrations were performed by plaque assay; serial dilutions were used to infect Vero A/T cells for 1 h. Following this, cells were overlaid with DMEM containing 2 % FCS, and 1.2 % Avicel®. After 72 h, the overlay was removed, and the monolayer washed and fixed with 100 % methanol. Monolayers were stained with a solution of 25 % (v/v) methanol and 0.5 % (w/v) Crystal Violet, then washed with water, and plaques were enumerated.

### 2.6. Statistical analysis

Viral titre data was log transformed and differences between sample types were analysed using 1-way analyses of variance (ANOVA) and Tukey's multiple comparison test.

## 3. Results and discussion

### 3.1. Uptake and release efficiencies of $Cu^{2+}$ exchanged pigment

To determine whether our novel coatings, based on smart-release cation-exchange pigments could be rendered antiviral through the incorporation copper (II) ions, we generated a $Cu^{2+}$-exchanged analogue, which was subsequently dispersed in an ethanolic solution of PVB to produce a model paint. To confirm the smart-release properties of the $Cu^{2+}$ loaded CEP, where cation exchange with an external electrolyte of high ionic strength will liberate stored $Cu^{2+}$ from the pigment, quantification of the uptake and release of $Cu^{2+}$ was carried out as described in Section 2. During pigment preparation by dispersion of as-received Amberlite 120 $H^+$ resin in a 0.2 M $CuSO_4$ solution, determination of the residual concentration of $Cu^{2+}$ (aq) in the post-exchange supernatant confirmed a pigment $Cu^{2+}$ cation capacity of 0.9 mmol/g. This empirically determined value is in full agreement with the anticipated cation exchange capacity of 1.8 meq/g previously quoted for this material. A subsequent back exchange experiment carried out by dispersing 1 g of fine, milled $Cu^{2+}$-CEP powder in 10 $cm^3$ of dilute sulphuric acid and subsequent determination of $Cu^{2+}$ concentration in solution after 2 h stirring demonstrated that 0.62 mmol/g of the stored $Cu^{2+}$ was released through the cation exchange process. The same experiment repeated in the presence of distilled water showed that <5 % of the stored $Cu^{2+}$ was liberated into solution, thus validating the notion of a triggered release of the anti-viral agent stored within the pigment.

### 3.2. Antiviral activities of various surfaces

To investigate the antiviral capacity of different materials, SARS-CoV-2 virions in DMEM were incubated on surfaces for 4 h, then residual titres of live virus calculated. To establish baseline parameters, the antiviral capacity of a copper surface was assessed. As expected given its well documented antiviral activity, copper resulted in a drop (3log10) in viral titres compared to a control (blank) well, while steel did not result in any reduction in titre at all (Fig. 1). Biological fluids such as saliva naturally contain proteins, we therefore included 2 % FCS in some samples to act as an organic soil load that mimics these proteins, a standard practice for testing disinfection of inanimate, nonporous environmental surfaces [34]. Surprisingly, the addition of 2 % FCS completely inhibited the antiviral efficacy of the copper (Fig. 1). All subsequent experiments were therefore conducted in the presence of 2 % FCS to allow for more stringent testing and to better mimic salivary droplets.

Having established baseline activity, the anti-viral action of copper-containing, PVB-based coatings applied to stainless steel substrates were tested (Fig. 2). A PVB composite coating containing 56 wt/% of dispersed $Cu^{2+}$-CEP pigment was compared with a coating based on a metallic Cu powder additive at the same loading (i.e. 5 g of pigment dispersed in 25 g of ethanolic PVB solution). The latter showed no efficacy against the virus, whereas the $Cu^{2+}$-CEP pigment loaded PVB coated surface showed a highly significant reduction (>6 log) of viral titre in comparison to a blank well, or control PVB coating lacking a copper-based pigment. Impressively, the $Cu^{2+}$-CEP system showed far greater efficacy against virus in the presence of 2 % FCS, than achieved with pure metallic copper against virus lacking FCS (>6 log reduction vs ~3 log reduction). A control experiment was carried out to determine whether any antiviral activity could be ascribed to $Cu^{2+}$ leaching out of the paint and inactivating the virus during the titration stages. Media without virus was added to the surface for 4 h, then rinsed off, and mixed with a known concentration of live virus, before virus titration as normal. No antiviral activity occurred, demonstrating that inactivation was predominantly occurring on the surface of the paint itself, and not during subsequent analysis (Supplementary Fig. 1).

A question arises as to why there is such a difference in antiviral efficiency between PVB coatings containing dispersions of Cu powder as opposed to $Cu^{2+}$–CEP, given that Cu species should be present in each. One explanation with respect to the inefficiency of the metallic Cu powder pigmented system could be the limited exposure of the Cu particles at the surface of the coating. It is possible that the PVB has enveloped most of the available powder and thereby limited contact to

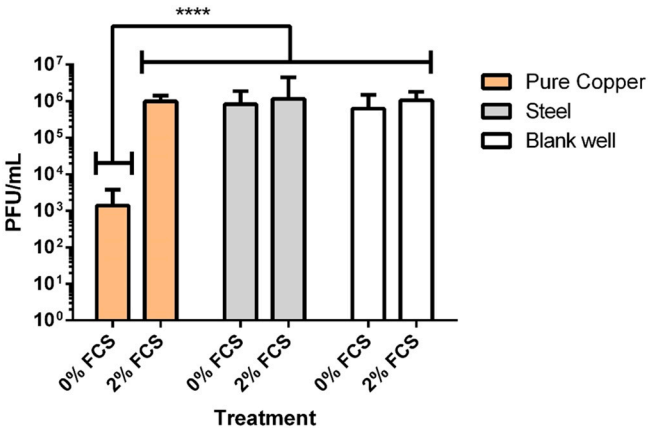


**Fig. 1.** Antiviral activities measured for steel, pure copper and blank wells in the presence and absence of FCS, as determined by plaque titration after 4 h of incubation. Data represents geometric means with 95 % confidence intervals, N = 4, **** = P < 0.0001 (ANOVA with Tukey's multiple comparison test). Limit of detection = 20 PFU/mL.

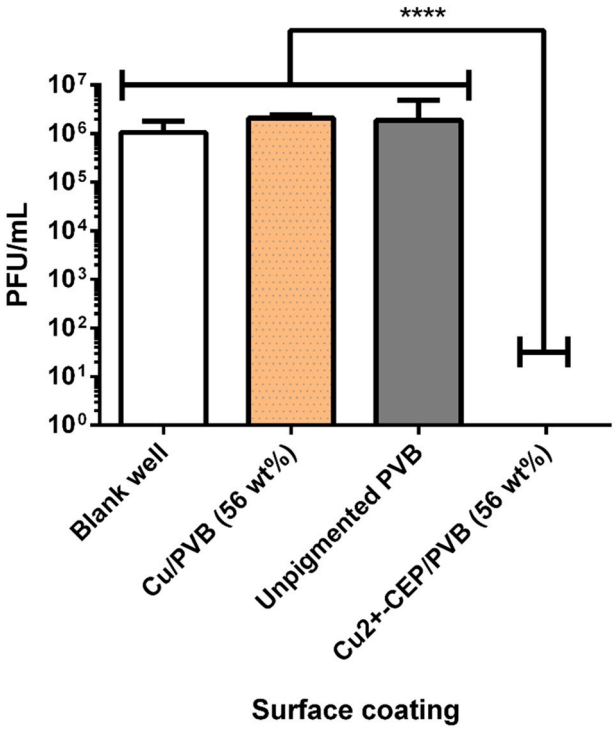


**Fig. 2.** Antiviral activities of various copper-based organic coatings using 2 % FCS virus stocks determined by plaque assay after 4 h of incubation. Data represents geometric means with 95 % confidence intervals, N = 4, **** = P < 0.0001 (ANOVA with Tukey's multiple comparison test). Limit of detection = 20 PFU/mL.

the Cu surface and subsequent release of ions. The inability of the bare Cu substrate to fully inactive the virus despite having the largest availability of Cu with respect to all the samples, suggests a limiting factor associated with the surface and/or availability of Cu species. Other works have reported the time dependant antiviral capacity of Cu and Cu alloyed surfaces in which a reduction in efficiencies is observed when these surfaces were exposed to air and the subsequent oxidation of the Cu surfaces.

### 3.3. Antiviral efficiency of $Cu^{2+}$ exchanged pigment

Based on the profound antiviral response observed by the $Cu^{2+}$-CEP system, an investigation as to whether a critical pigment loading exists with respect to antiviral action was conducted. Fig. 3 shows the measured viral titres for 6 CEP systems of varying pigment loading (11–56 % w/w based on a dry CEP-PVB composite film) alongside a non-pigmented PVB reference. A critical pigment loading threshold exists between 42 and 50 wt% of the $Cu^{2+}$-CEP/PVB system at which point the antiviral action almost entirely stops.

This critical threshold can be attributed to the availability of $Cu^{2+}$ ions which is governed by the exposure of pigment particles at the coating surface. Like the metal Cu pigment analogue, at a 42 % loading, there is insufficient direct exposure of the pigment particles at the coating surface, and the release of Cu species is limited. A schematic representation of the coating and virus interface is provided in Fig. 4. Without direct exposure of the pigment, ion exchange and release of $Cu^{2+}$ (either from $H^+$ or other relevant reactive cationic species e.g. $Na^+$) will be limited and the antiviral action diminished. It should also be noted that if this smart-release technology is deployed as a coating which can bestow anti-viral activity to high touch surfaces, such as door handles, railing, push plates etc., then ion-exchange triggered liberation of the stored $Cu^{2+}$ will take place in palmar or fingermark deposits which will contain inorganic group I chlorides. [35].

## 4. Discussion

Several antiviral mechanisms of Cu have been proposed but an exact understanding remains elusive. Generally, the virucidal properties of Cu are primarily attributed to the release of both $Cu^+$ and $Cu^{2+}$ species. The most consistently reported mechanisms is associated with the production of redox radicals, specifically, reactive oxygen species (ROS) generated from the cycling of Cu ion states, as shown in the Haber-Weiss and Fenton reactions (Eqs. (2) & (3)) [36]

$$Cu^{2+} + \dot{O}_2 \rightarrow Cu^{+} + O_2 \quad (2)$$

$$Cu^{+} + H_2O_2 \rightarrow Cu^{2+} + OH^{-} + \dot{O}H \quad (3)$$

Release of ROS leads to damage of the virus lipids, proteins and nucleic acids, thereby destroying the capability to infect or replicate and rendering the virus inactive [37]. In other studies, the action of ROS has been shown to interact and degrade the virus envelope.

The exchanged pigment will be a source of $Cu^{2+}$ only, which would suggest that the primary antiviral mechanism of the composite PVB coatings investigated here is associated with $Cu^{2+}$ rather than $Cu^+$. Other studies have demonstrated the direct antiviral action of $Cu^{2+}$ ions, whereby they form complexes with biomolecules or displace metal ions in specific metalloproteins, causing protein degradation/denaturation and ultimately inactivation [35]. Evidence of a combined mechanism in which virus morphology is irreversibly changed, inducing a disintegration of the virus envelope and dispersal of the spike proteins has also been reported [38]. This change and subsequent inactivation was attributed to the action of both $Cu^+$ and $Cu^{2+}$ ions and assisted by ROS generation. A schematic representation of both potential antiviral mechanisms is illustrated in Fig. 5.

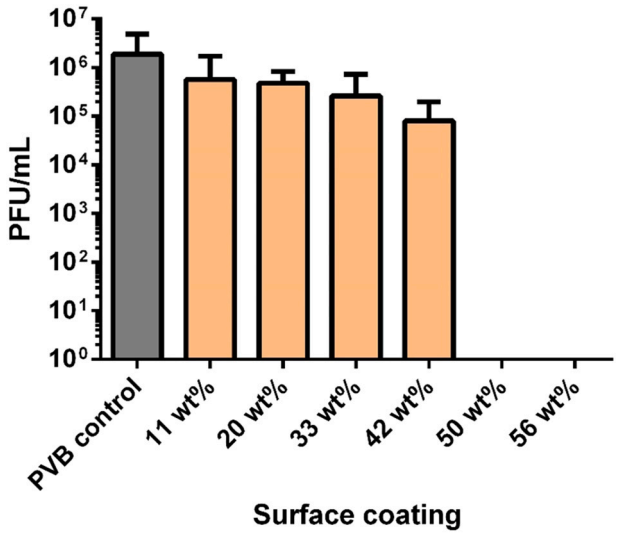


**Fig. 3.** Antiviral activities measured for PVB coatings containing varying $Cu^{2+}$-CEP pigment loadings applied to stainless steel substrates, compared with an unpigmented PVB reference, using 2 % FCS virus determined by PFU titre post 4 h of incubation. Data represents geometric means with 95 % confidence intervals, N = 4. Limit of detection = 20 PFU/mL.

## 5. Conclusion

A simple organic coating based on $Cu^{2+}$ exchanged resin pigment ($Cu^{2+}$-CEP) dispersed in a polymer binder and applied to stainless steel substrates demonstrates potent activity against an enveloped virus (SARS-CoV-2). Furthermore, the $Cu^{2+}$-CEP additive, when loaded to a critical amount, is capable of inactivating >6log10 of virus even in the presence of a soil load. In contrast, metallic copper surfaces and an organic coating containing dispersed metallic copper surfaces or Cu powder are significantly less effective under identical conditions. The approach of using a very basic paint system, based on a polymer binder embedded with “smart release” pigment containing an anti-viral agent which is liberated by ion-exchange, holds significant promise as a cost effective and rapidly deployed coating to confer virus killing capability to high touch surfaces.

Supplementary data to this article can be found online at https://doi.org/10.1016/j.porgcoat.2022.107135.

## Funding sources

This work was supported by funding from the EPSRC (EP/N020863/1), MRC (MR/V028448/1, MR/S00971X/1), and Accelerate Wales.

## CRediT authorship contribution statement

Zack Saud: investigation, methodology, visualisation, writing – original draft. Calvin Richards: investigation, methodology, visualisation, writing – review & editing. Geraint Williams: conceptualisation, funding acquisition, project administration, supervision, writing – original draft. Richard Stanton: conceptualisation, funding acquisition, methodology, project administration, supervision, writing – review & editing.

## Declaration of competing interest

The authors declare that they have no known competing financial interests or personal relationships that could have appeared to influence the work reported in this paper.

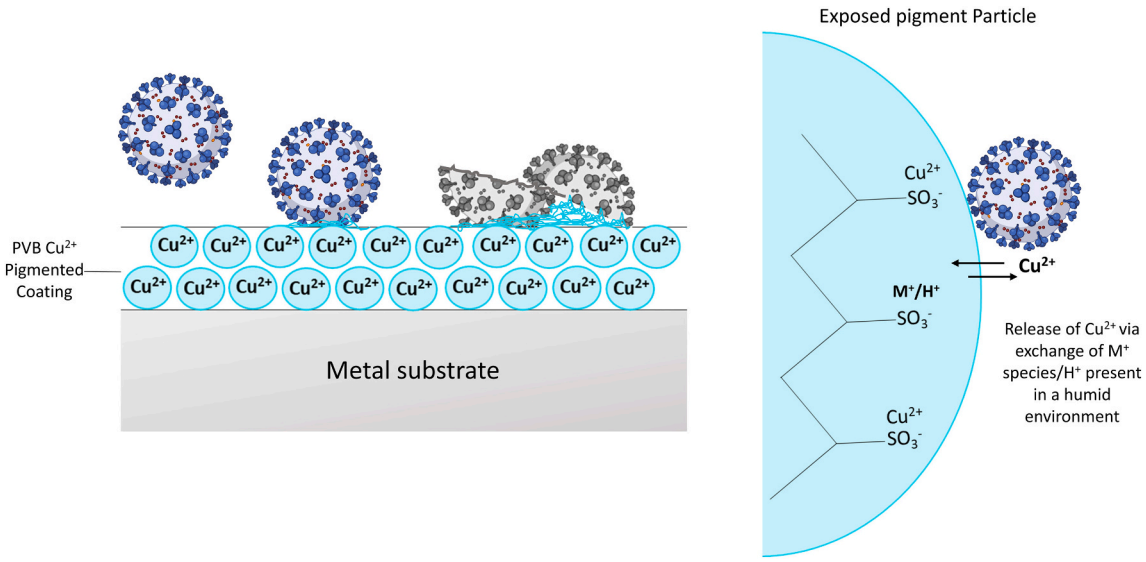


**Fig. 4.** Schematic representation of the $Cu^{2+}$-CEP/PVB composite coating interface along with associated cation-exchange anti-viral agent release mechanism.

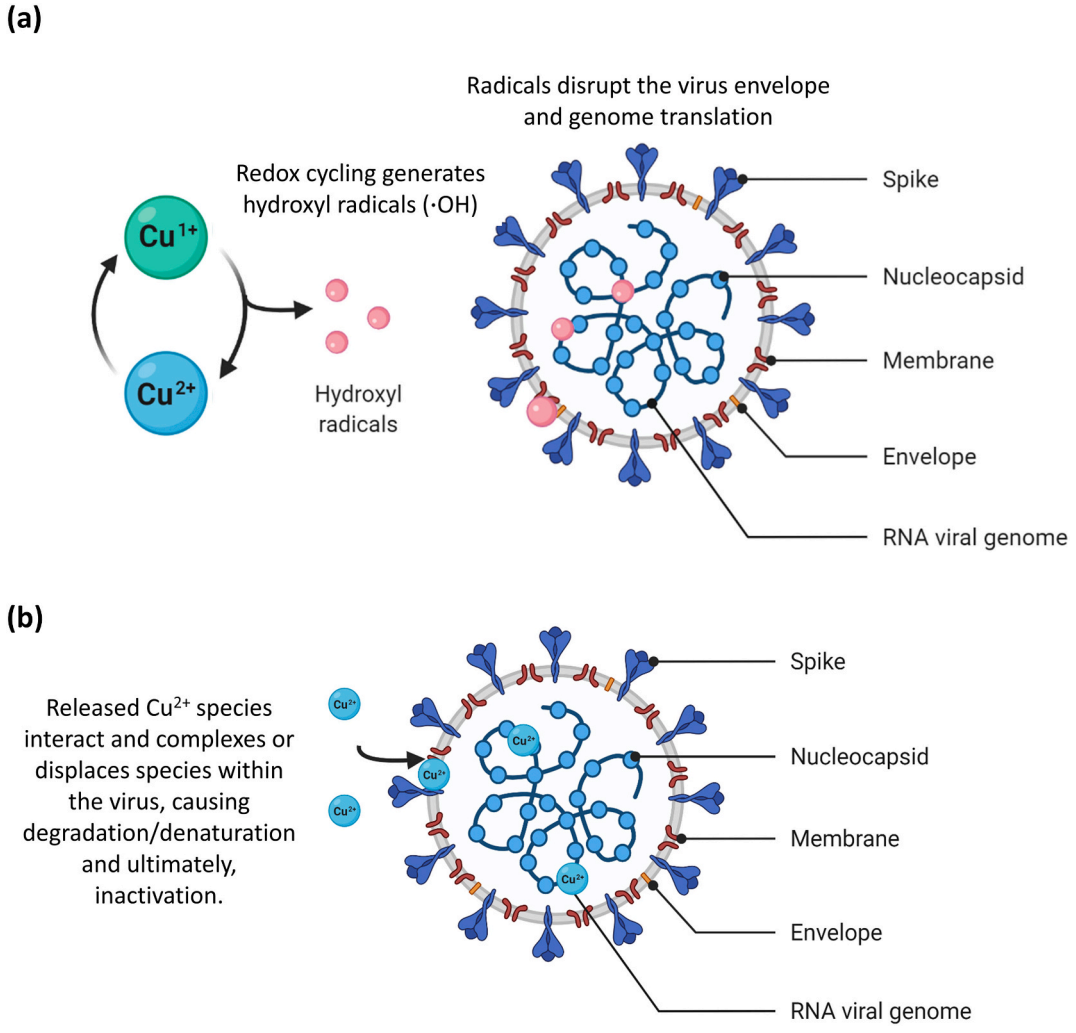


**Fig. 5.** Schematic diagrams showing the proposed antiviral mechanisms associated with a) the ROS production and virus attack by Cu ion redox reactions and b) direct interaction of $Cu^{2+}$ with virions.

## Data availability

No data was used for the research described in the article.

## References


[1] D.M. Morens, A.S. Fauci, Emerging pandemic diseases: how we got to COVID-19, Cell 182 (5) (2020) 1077–1092, https://doi.org/10.1016/J.CELL.2020.08.021.

[2] P. Zhou, X.-L. Yang, X.-G. Wang, B. Hu, L. Zhang, W. Zhang, H.-R. Si, Y. Zhu, B. Li, C.-L. Huang, H.-D. Chen, J. Chen, Y. Luo, H. Guo, R.-D. Jiang, M.-Q. Liu, Y. Chen, X.-R. Shen, X. Wang, X.-S. Zheng, K. Zhao, Q.-J. Chen, F. Deng, L.-L. Liu, B. Yan, F.-X. Zhan, Y.-Y. Wang, G.-F. Xiao, Z.-L. Shi, A pneumonia outbreak associated with a new coronavirus of probable bat origin, Nature 579 (2020) 270–273, https://doi.org/10.1038/s41586-020-2012-7.

[3] T. Bedford, A.L. Greninger, P. Roychoudhury, L.M. Starita, M. Famulare, M. L. Huang, A. Nalla, G. Pepper, A. Reinhardt, H. Xie, L. Shrestha, T.N. Nguyen, A. Adler, E. Brandstetter, S. Cho, D. Giroux, P.D. Han, K. Fay, C.D. Frazar, M.L. Z. Suchsland, Cryptic transmission of SARS-CoV-2 in Washington State, Science 370 (6516) (2020) 571–575, https://doi.org/10.1126/science.abc0523.

[4] M. Sironi, S.E. Hasnain, B. Rosenthal, T. Phan, F. Luciani, M.A. Shaw, M.A. Sallum, M.E. Mirhashemi, S. Morand, F. González-Candelas, SARS-CoV-2 and COVID-19: a genetic, epidemiological, and evolutionary perspective, Infect. Genet. Evol. 84 (2020), 104384, https://doi.org/10.1016/J.MEEGID.2020.104384.

[5] H.A. Rothan, S.N. Byrareddy, The epidemiology and pathogenesis of coronavirus disease (COVID-19) outbreak, J. Autoimmun. 109 (2020), 102433, https://doi.org/10.1016/j.jaut.2020.102433.

[6] Y.C. Wu, C.S. Chen, Y.J. Chan, The outbreak of COVID-19: an overview, Journal of the Chinese Medical Association 2020 83(3) (2020) 217–220, https://doi.org/10.1097/JCMA.0000000000000270.

[7] S. Kannan, P. Shaik Syed Ali, A. Sheeza, K. Hemalatha, COVID-19 (Novel Coronavirus 2019) - recent trends, Eur. Rev. Med. Pharmacol. Sci. 24 (4) (2020) 2006–2011, https://doi.org/10.26355/eurrev_202002_20378.

[8] Centers for Disease Control and Prevention, Science Brief: SARS-CoV-2 and Surface (Fomite) Transmission for Indoor Community Environments, Available at, https://www.cdc.gov/coronavirus/2019-ncov/more/science-and-research/surface-transmission.html. Accessed 03 June 2022.

[9] M.O. Aydogdu, E. Altun, E. Chung, G. Ren, S. Homer-Vanniasinkam, B. Chen, M. Edirisinghe, Surface interactions and viability of coronaviruses, J. R. Soc. Interface 18 (2021), 20200798, https://doi.org/10.1098/rsif.2020.0798.

[10] N. van Doremalen, T. Bushmaker, D.H. Morris, M.G. Holbrook, A. Gamble, B. N. Williamson, A. Tamin, J.L. Harcourt, N.J. Thornburg, S.I. Gerber, J.O. Lloyd-Smith, E. de Wit, V.J. Munster, Aerosol and surface stability of SARS-CoV-2 as compared with SARS-CoV-1, N. Engl. J. Med. 382 (16) (2020) 1564–1567, https://doi.org/10.1056/NEJMc2004973.

[11] S. Behzadinasab, A.W.H. Chin, M. Hosseini, L.L.M. Poon, W.A. Ducker, SARS-CoV-2 virus transfers to skin through contact with contaminated solids, Sci. Rep. 11 (1) (2021) 22868, https://doi.org/10.1038/s41598-021-00843-0.

[12] S.F. Sia, L.M. Yan, A.W.H. Chin, K. Fung, K.T. Choy, A.Y.L. Wong, P. Kaewpreedee, R.A.P.M. Perera, L.L.M. Poon, J.M. Nicholls, M. Peiris, H.L. Yen, Pathogenesis and transmission of SARS-CoV-2 in golden hamsters, Nature 583 (7818) (2020) 834–838, https://doi.org/10.1038/s41586-020-2342-5.

[13] M. Minoshima, Y. Lu, T. Kimura, R. Nakano, H. Ishiguro, Y. Kubota, K. Hashimoto, K. Sunada, Comparison of the antiviral effect of solid-state copper and silver compounds, J. Hazard. Mater. 312 (2016) 1–7, https://doi.org/10.1016/j.jhazmat.2016.03.023.

[14] V. Govind, S. Bharadwaj, M.R. Sai Ganesh, J. Vishnu, K.V. Shankar, B. Shankar, R. Rajesh, Antiviral properties of copper and its alloys to inactivate covid-19 virus: a review, BioMetals 34 (2021) 1217–1235, https://doi.org/10.1007/s10534-021-00339-4.

[15] M. Vincent, R.E. Duval, P. Hartemann, M. Engels-Deutsch, Contact killing and antimicrobial properties of copper, J. Appl. Microbiol. 124 (5) (2018) 1032–1046, https://doi.org/10.1111/jam.13681.

[16] Y. Fujimori, T. Sato, T. Hayata, T. Nagao, M. Nakayam, T. Nakayam, R. Sugamat, K. Suzuki, Novel antiviral characteristics of nanosized copper(i) iodide particles showing inactivation activity against 2009 pandemic H1N1 influenza virus, Appl. Environ. Microbiol. 78 (4) (2012) 951–955, https://doi.org/10.1128/AEM.06284-11.

[17] S. Jung, J.Y. Yang, E.Y. Byeon, D.G. Kim, D.G. Lee, S. Ryoo, S. Lee, C.W. Shin, H. W. Jang, H.J. Kim, S. Lee, Copper-coated polypropylene filter face mask with SARS-CoV-2 antiviral ability, Polymers (Basel) 13 (9) (2021) 1367, https://doi.org/10.3390/polym13091367.

[18] G. Borkow, J. Gabbay, Putting copper into action: copper-impregnated products with potent biocidal activities, FASEB J. 18 (14) (2004) 1728–1730, https://doi.org/10.1096/fj.04-2029fje.

[19] J.D. Ranford, P.J. Sadler, D.A. Tocher, Cytotoxicity and antiviral activity of transition-metal salicylato complexes and crystal structure of Bis (diisopropylsalicylato)(1,10-phenanthroline)copper(II), J. Chem. Soc. Dalton Trans. 22 (1993) 3393–3399, https://doi.org/10.1039/DT9930003393.

[20] S. Behzadinasab, A. Chin, M. Hosseini, L. Poon, W.A. Ducker, A surface coating that rapidly inactivates SARS-CoV-2, ACS Appl. Mater. Interfaces 12 (31) (2020) 34723–34727, https://doi.org/10.1021/acsami.0c11425.

[21] S. Behzadinasab, M.D. Williams, M. Hosseini, L.L.M. Poon, A.W.H. Chin, J. O. Falkinham III, W.A. Ducker, Transparent and sprayable surface coatings that kill drug-resistant bacteria within minutes and inactivate SARS-CoV-2 virus, ACS Appl. Mater. Interfaces 13 (46) (2021) 54706–54714, https://doi.org/10.1021/acsami.1c15505.

[22] K. Imai, H. Ogawa, V.N. Bui, H. Inoue, J. Fukuda, M. Ohba, Y. Yamamoto, K. Nakamura, Inactivation of high and low pathogenic avian influenza virus H5 subtypes by copper ions incorporated in zeolite-textile materials, Antivir. Res. 93 (2) (2012) 225–233, https://doi.org/10.1016/j.antiviral.2011.11.017.

[23] K.R. Bright, E.E. Sicairos-Ruelas, P.M. Gundy, C.P. Gerba, Assessment of the antiviral properties of zeolites containing metal ions, Food Environ.Virol. 1 (1) (2009) 37–41, https://doi.org/10.1007/s12560-008-9006-1.

[24] J. Cui, R. Yeasmin, Y. Shao, H. Zhang, H. Zhang, J. Zhu, Fabrication of Ag+, Cu2+, and Zn2+ ternary ion-exchanged zeolite as an antimicrobial agent in powder coating, Ind. Eng. Chem. Res. 59 (2) (2020) 751–762, https://doi.org/10.1021/acs.iecr.9b05338.

[25] S. Bohm, H.N. McMurray, S.M. Powell, D.A. Worsley, Novel environment friendly corrosion inhibitor pigments based on naturally occurring clay minerals, Mater. Corros. 52 (2001) 896–903.

[26] G. Williams, H.N. McMurray, D.A. Worsley, Cerium (III) inhibition of corrosion driven organic coating delamination studied using a scanning kelvin probe technique, J. Electrochem. Soc. 149 (2002) B154–B162.

[27] G. Williams, H.N. McMurray, M.J. Loveridge, Inhibition of corrosion-driven organic coating disbondment on galvanised steel by smart release group II and Zn (II)-exchanged bentonite pigments, Electrochim. Acta 55 (5) (2010) 1740–1748, https://doi.org/10.1016/j.electacta.2009.10.059.

[28] G. Williams, S. Geary, H.N. McMurray, Smart release corrosion inhibitor pigments based on organic ion-exchange resins, Corros. Sci. 57 (2012) 139–147, https://doi.org/10.1016/j.corsci.2011.12.024.

[29] C.A.J. Richards, H.N. McMurray, G. Williams, Smart-release inhibition of corrosion driven organic coating failure on zinc by cationic benzotriazole based pigments, Corros. Sci. 154 (2019) 101–110, https://doi.org/10.1016/J.CORSCI.2019.04.005.

[30] S.J. Rihn, A. Merits, S. Bakshi, M.L. Turnbull, A. Wickenhagen, A.J.T. Alexander, S. Mahalingam, A plasmid DNA-launched SARS-CoV-2 reverse genetics system and coronavirus toolkit for COVID-19 research, PLoS Biol. 19 (2) (2021), e3001091, https://doi.org/10.1371/journal.pbio.3001091.

[31] D. Guspita, A. Ulianas, Optimization of complex NH3 with Cu2+ ions to determine levels of ammonia by UV-Vis spectrophotometer, J. Phys. Conf. Ser. 1481 (1) (2020), 012040, https://doi.org/10.1088/1742-6596/1481/1/012040.

[32] L.N. Trevani, J.C. Roberts, P.R. Tremaine, Copper(II)-ammonia complexation equilibria in aqueous solutions at temperatures from 30 to 250°C by visible spectroscopy, J. Solut. Chem. 30 (7) (2001) 585–622, https://doi.org/10.1023/A:1010453412802.

[33] G. Williams, H.N. McMurray, Latent fingermark visualisation using a scanning Kelvin probe, Forensic Sci. Int. 167 (2007) 102–109.

[34] ASTM International, ASTM E1053–20. Standard practice to assess virucidal activity of chemicals intended for disinfection of inanimate, nonporous environmental surfaces, 2020, https://doi.org/10.1520/E1053-20. https://www.astm.org/Standards/E1053.htm.

[35] T. Ishida, Antiviral activities of Cu2+ ions in viral prevention, replication, RNA degradation, and for antiviral efficacies of lytic virus, ROS-mediated virus, copper chelation, World Sci.News 99 (2018) 148–168.

[36] J.M. Rifkind, Y.A. Shin, J.M. Heim, G.L. Eichhorn, Cooperative disordering of single-stranded polynucleotides through copper crosslinking, Biopolymers 15 (1976) 1879–1902.

[37] Y.-N. Chang, M. Zhang, L. Xia, J. Zhang, G. Xing, The toxic effects and mechanisms of CuO and ZnO nanoparticles, Materials 5 (12) (2012) 2850–2871.

[38] S.L. Warnes, Z.R. Little, C.W. Keevil, Human coronavirus 229E remains infectious on common touch surface materials, mBio 6 (6) (2015), e01697-15, https://doi.org/10.1128/mBio.01697-15.